OXFORD

Human Molecular Genetics, 2023, Vol. 32, 13, 2152–2161
https://doi.org/10.1093/hmg/ddad050
Advance access publication date 31 March 2023
Original Article

SOX7 deficiency causes ventricular septal defects through its effects on endocardial-to-mesenchymal transition and the expression of *Wnt4* and *Bmp2*

Andrés Hernández-García[1], Katherine E. Pendleton[1], Sangbae Kim[1], Yumei Li[1], Bum J. Kim[1], Hitisha P. Zaveri[1], Valerie K. Jordan[2], Aliska M. Berry[1], M. Cecilia Ljungberg[3,4], Rui Chen[1], Rainer B. Lanz[5,6] and Daryl A. Scott[1,2,*]

[1]Department of Molecular and Human Genetics, Baylor College of Medicine, Houston, TX 77030, USA
[2]Department of Molecular Physiology and Biophysics, Baylor College of Medicine, Houston, TX 77030, USA
[3]Department of Pediatrics, Baylor College of Medicine, Houston, TX 77030, USA
[4]Jan and Dan Duncan Neurological Research Institute at Texas Children's Hospital, Houston, TX 77030, USA
[5]Department of Molecular & Cellular Biology, Baylor College of Medicine, Houston, TX 77030, USA
[6]Quantitative and Computational Biosciences, Baylor College of Medicine, Houston, TX 77030, USA

*To whom correspondence should be addressed. Tel: +1 7132037242; Email: dscott@bcm.edu

Abstract

SOX7 is a transcription factor-encoding gene located in a region on chromosome 8p23.1 that is recurrently deleted in individuals with ventricular septal defects (VSDs). We have previously shown that *Sox7*$^{-/-}$ embryos die of heart failure around E11.5. Here, we demonstrate that these embryos have hypocellular endocardial cushions with severely reduced numbers of mesenchymal cells. Ablation of *Sox7* in the endocardium also resulted in hypocellular endocardial cushions, and we observed VSDs in rare E15.5 *Sox7*$^{flox/-}$;Tie2-Cre and *Sox7*$^{flox/flox}$;Tie2-Cre embryos that survived to E15.5. In atrioventricular explant studies, we showed that SOX7 deficiency leads to a severe reduction in endocardial-to-mesenchymal transition (EndMT). RNA-seq studies performed on E9.5 *Sox7*$^{-/-}$ heart tubes revealed severely reduced *Wnt4* transcript levels. *Wnt4* is expressed in the endocardium and promotes EndMT by acting in a paracrine manner to increase the expression of *Bmp2* in the myocardium. Both *WNT4* and *BMP2* have been previously implicated in the development of VSDs in individuals with 46,XX sex reversal with dysgenesis of kidney, adrenals and lungs (SERKAL) syndrome and in individuals with short stature, facial dysmorphism and skeletal anomalies with or without cardiac anomalies 1 (SSFSC1) syndrome, respectively. We now show that *Sox7* and *Wnt4* interact genetically in the development of VSDs through their additive effects on endocardial cushion development with *Sox7*$^{+/-}$;*Wnt4*$^{+/-}$ double heterozygous embryos having hypocellular endocardial cushions and perimembranous and muscular VSDs not seen in their *Sox7*$^{+/-}$ and *Wnt4*$^{+/-}$ littermates. These results provide additional evidence that SOX7, WNT4 and BMP2 function in the same pathway during mammalian septal development and that their deficiency can contribute to the development of VSDs in humans.

Introduction

8p23.1 microdeletion syndrome is caused by a non-allelic homologous recombination mediated by low-copy repeats flanking a ~3.4 Mb region of DNA (1). Recurrent deletions of this region are associated with a variety of neurodevelopmental phenotypes, dysmorphic features, a high incidence of congenital heart defects (CHDs), and congenital diaphragmatic hernia (2–5). Haploinsufficiency of *GATA4*, one of the genes located in this region, is sufficient to cause CHD (6,7). However, published reports suggested that the spectrum of cardiac defects seen in individuals with 8p23.1 deletions is more severe than that seen in individuals with heterozygous pathogenic variants in *GATA4* (1).

SOX7 is located within 1 Mb of *GATA4* in the recurrently deleted region on chromosome 8p23.1 and has been hypothesized to contribute to the development of CHD (1). This hypothesis is supported by a report from Huang *et al*. in which they describe a four-generation family in which CHDs co-segregated with a c.310C>T, p.(Gln104*) [NM_031439.4] premature stop variant in *SOX7* (8). Ventricular septal defects (VSDs) were among the most common forms of CHD seen in affected members of this family.

Animal models provide further support for the role of SOX7 in cardiovascular development. In *Xenopus*, injection of RNAs encoding *Sox7* leads to the nodal-dependent expression of markers of cardiogenesis in animal cap explants, whereas injection of morpholinos directed against *Sox7* leads to a partial inhibition of cardiogenesis *in vivo* (9). In zebrafish, simultaneous knockdown of *Sox7* and *Sox18* leads to a severe loss of the arterial identity of the presumptive aorta leading to dysmorphogenesis of the proximal aorta, the development of arteriovenous shunts, and a lack of circulation in the trunk and tail (10,11).

In mice, ablation of *Sox7* results in defects in vascular remodeling. Specifically, *Sox7*$^{-/-}$ embryos die around E11.5 with failure of yolk sac vascular remodeling and dilated pericardial sacs suggestive of cardiovascular failure (12). Hong *et al*. have recently shown that *Sox7*$^{flox/flox}$;Nfatc1-Cre embryos have reduced mesenchymal cell numbers in their atrioventricular (AV) cushions at E9.5, E10.5 and E11.5 because of a defect in endocardial-to-mesenchymal transformation (EndMT), delayed fusion of ventricular septum with cardiac cushion at E13.5, and defects in the closure of the atrial septum at E14.5 (13). They went on to show that BMP2

Received: November 4, 2022. **Revised:** March 9, 2023. **Accepted:** March 27, 2023

signaling was downregulated in *Sox7*$^{flox/flox}$;Nfatc1-Cre AV canals at E9.5, that *Wnt4* is a downstream target of *Sox7*, and that WNT4 or BMP2 treatment partially rescued the EndMT defect caused by SOX7 deficiency (13).

Here, we confirm that systemic and endocardial-specific SOX7 deficiency leads to the development of hypocellular endocardial cushions and VSDs caused by a lack of EndMT in the developing AV canal. In a transcriptome analysis performed on E9.5 *Sox7*$^{-/-}$ heart tubes, and in RNA *in situ* hybridization (RNA-ISH) studies, we confirmed that SOX7 modulates the expression of *Wnt4* in the endocardium and *Bmp2* in the myocardium. We also show that *Sox7* and *Wnt4* interact genetically in the development of perimembranous and muscular VSDs through their additive effects on endocardial cushion development.

Results

Ablation of *Sox7* in the endocardium causes VSDs

Septal defects are among the most common forms of CHD associated with 8p23.1 microdeletions and SOX7 haploinsufficiency (1,8). *Sox7*$^{-/-}$ mouse embryos die around E11.5 (12), a time point that does not allow evaluation of the development of the AV septum. In an effort to overcome this limitation, we attempted to generate *Sox7*$^{flox/-}$;Tie-2 Cre embryos in which one *Sox7* allele was ablated systemically and the other was selectively ablated in endothelial cells, including the endocardium, using a transgenic Tie2-Cre which does not affect the expression of *Tie2* (14). Although most of these embryos died prior to E15.5, we were able to harvest two rare survivors at this time point. One of these embryos had normal cardiac anatomy, but the other had a VSD not seen in control littermates (Fig. 1A and B).

We then sought to generate mice in which *Sox7* was ablated only in endothelial cells. Similarly, the majority of *Sox7*$^{flox/flox}$;Tie2-Cre embryos died prior to E15.5. However, we were able to harvest one *Sox7*$^{flox/flox/}$;Tie2-Cre embryo at this time point. This embryo also had a VSD (Fig. 1C and C′). These results provide evidence that ablation of *Sox7* in the endocardium is sufficient to cause VSDs.

Systemic SOX7 deficiency leads to hypocellular AV endocardial cushions

Since the mesenchymal cells of the AV endocardial cushions will ultimately form the AV septum and its associated valves (15), we looked for differences in the development of the endocardial cushions between E10.5 *Sox7*$^{-/-}$ embryos and their wild-type littermates. Examination of sagittal sections through the AV endocardial cushions of *Sox7*$^{-/-}$ embryos revealed normal separation of the endocardium from the underlying myocardium. Furthermore, the size of the AV endocardial cushions in *Sox7*$^{-/-}$ embryos was comparable to those of their wild-type littermates (Fig. 2A and B). Although comparable in size, the AV endocardial cushions of E9.5/10.5 *Sox7*$^{-/-}$ embryos had severely reduced mesenchymal cell density when compared with those of their wild-type littermates ($P \leq 0.0001$; Fig. 2C).

Ablation of *Sox7* in the endocardium leads to hypocellular AV endocardial cushions

To confirm that the AV endocardial cushion hypocellularity seen in Sox7$^{-/-}$ embryos was due to decreased expression of SOX7 within endocardial cells, we examined embryos in which *Sox7* was ablated in the endocardium using a transgenic Tie2-Cre. Specifically, we examined sagittal sections through the AV endocardial cushions of E10.5 *Sox7*$^{flox/flox/}$;Tie2-Cre embryos and their *Sox7*$^{flox/+}$, *Sox7*$^{flox/flox}$ and *Sox7*$^{flox/+}$;Tie2-Cre littermate controls. We found that the endocardial cushions of E10.5 *Sox7*$^{flox/flox/}$;Tie2-Cre embryos had significantly reduced mesenchymal cell density compared with those of their control littermates (Fig. 2D–F). This suggests that the ablation of *Sox7* in the endocardium leads to hypocellularity of the AV endocardial cushions.

SOX7 deficiency leads to a decrease in EndMT

During septal development, a subset of endocardial cells in the AV canal undergoes EndMT to form mesenchymal cells, which migrate into the cardiac jelly between the endocardium and the myocardium (16,17). Hence, decreased levels of EndMT can lead to development of hypocellular AV endocardial cushions. To determine if a defect in EndMT could underlie the hypocellularity of the AV endocardial cushions seen in *Sox7*$^{-/-}$ embryos, we performed collagen gel AV canal explant studies. Briefly, the AV canals of *Sox7*$^{-/-}$ embryos and their wild-type littermates were harvested at E9.5, and the number of migrating mesenchymal cells emanating from the explants was counted after 48 h of collagen gel culture. These studies revealed significantly reduced numbers of migrating mesenchymal cells associated with *Sox7*$^{-/-}$ explants compared with wild-type explants ($P < 0.0001$, Fig. 2G–I). This suggests that a defect in EndMT is a major contributor to the development of the hypocellular AV endocardial cushions caused by ablation of *Sox7*.

RNA-seq analysis reveals alterations in genes associated with epithelial-to-mesenchymal transition with downregulation of *Wnt4* and *Bmp2*

Since *Sox7* encodes a DNA binding transcription factor, it is reasonable to assume that it regulates the transcription of key genes during heart development (18,19). To identify putative SOX7 target genes in an unbiased manner, we compared the RNA-seq transcriptomes of pooled heart tubes from *Sox7*$^{-/-}$ embryos harvested at E9.5 to those of their wild-type littermates. Using the Bioconductor DESeq2 package, we found 722 differentially expressed genes (*P*-value < 0.001 and absolute fold change > 2; Supplementary Material, Table S1). We then queried the Molecular Signature Database (MSigDB) with Gene Set Enrichment Analysis software (20) to determine whether the *Sox7*$^{-/-}$ differentially expressed genes show statistically significant, concordant differences between biological states. Figure 3A shows ranked overlaps with the MSigDB Hallmark gene sets, which summarize and represent well-defined phenotypes. Ingenuity Canonical Pathway analysis also revealed enrichments for the canonical pathways 'Glycolysis', 'Nitric Oxide Signaling in the Cardiovascular System' and 'Regulation of the Epithelial-Mesenchymal Transition Pathway'. Overlapping genes for each Hallmark gene set are shown in Supplementary Material, Table S2. 'Cardiovascular System Development and Function' was the top enrichment (*P*-value 3.42e-16) for disease and function annotations.

Among the differentially expressed genes with known roles in EndMT, we noted that *Wnt4* expression was downregulated (Fig. 3B). WNT4 is expressed in the endocardium and promotes EndMT by acting in a paracrine manner to increase the expression of BMP2 in the myocardium (21). Consistent with these findings, we found that *Bmp2* transcript levels were also diminished in *Sox7*$^{-/-}$ embryonic hearts, although to a lesser degree that did not meet criteria for inclusion among the list of differentially expressed genes (Fig. 3B).

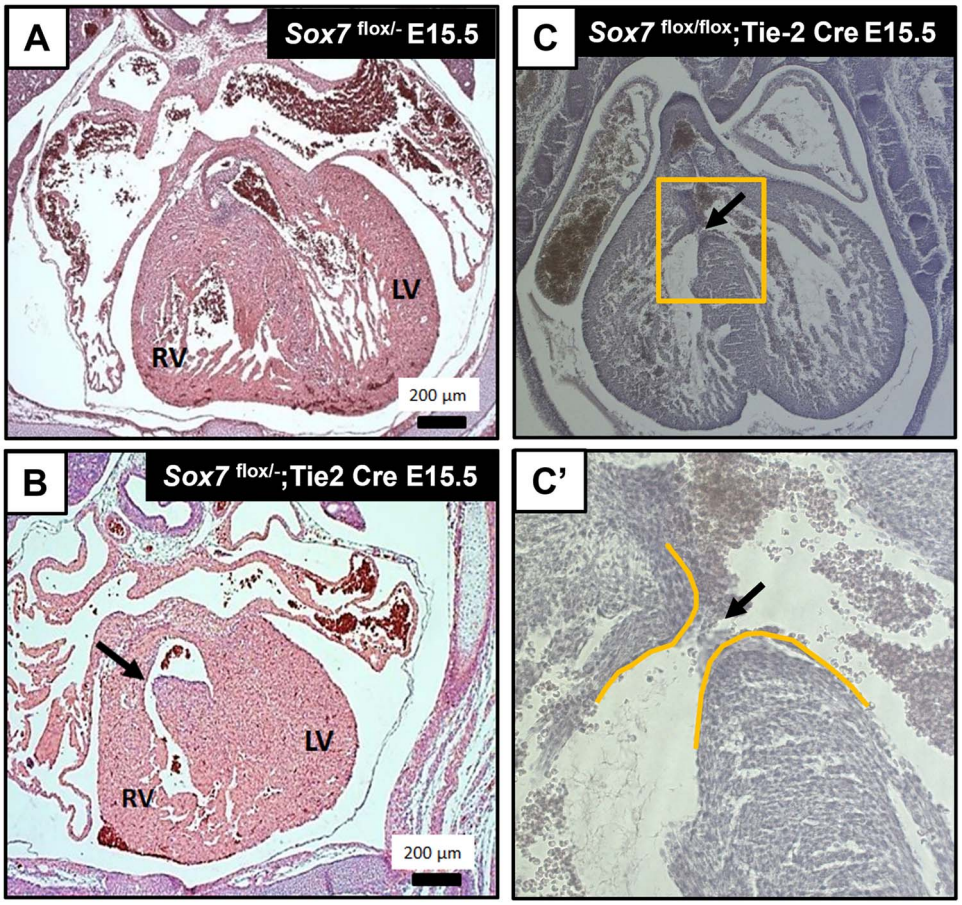

Figure 1. SOX7 deficiency in the endocardium causes VSDs. (**A**–**B**) By E15.5, the right and left ventricles are separated by the interventricular septum in C57BL/6 mice. In contrast, one of two rare $Sox7^{flox/-}$;Tie-2 Cre embryos that survived to E15.5 had a VSD (black arrow in B). (**C**) A single $Sox7^{flox/flox}$;Tie-2 Cre embryo was harvested at E15.5. This embryo also had a VSD (black arrow). (**C'**) Magnified image of the area marked by the yellow rectangle in (C). In this view, the endocardium is marked with yellow lines and the ventricular septal defect is marked by the black arrow. Blood cells are seen between the endocardial layers. LV = left ventricle, RV = right ventricle.

Wnt4 and *Bmp2* transcript levels are decreased in the AV canals of $Sox7^{-/-}$ mice

To confirm the downregulation of *Wnt4*, we compared its transcript level in the AV canals of $Sox7^{-/-}$ and wild-type embryos at E9.5 by RNA-ISH. We found that *Wnt4* transcript levels were reduced in the endocardium of AV canal sections obtained from E9.5 $Sox7^{-/-}$ embryos compared with those obtained from their wild-type littermates (Fig. 3C–D). The level of *Bmp2* transcripts also appeared to be reduced in the myocardium of the AV canals of $Sox7^{-/-}$ embryos (Fig. 3E–F). These results are consistent with a model in which SOX7 positively regulates *Wnt4* expression in the endocardium. WNT4 then acts in a paracrine fashion to upregulate expression of *Bmp2* in the myocardium which has a positive effect on EndMT (Fig. 3G).

Sox7 and *Wnt4* interact genetically in the development of VSDs

To provide additional evidence that SOX7 and WNT4 function within a common pathway during cardiac development, we looked for evidence that *Sox7* and *Wnt4* interact genetically in the development of VSDs. Specifically, we crossed $Sox7^{+/-}$ mice with mice bearing a single *Wnt4* eGFPCreERT2 (GCE) knock-in/knock-out allele ($Wnt4^{+/-}$) to generate $Sox7^{+/-}$;$Wnt4^{+/-}$ double heterozygous embryos and mice. At E15.5/E16.5, wild-type, $Sox7^{+/-}$, $Wnt4^{+/-}$, and $Sox7^{+/-}$;$Wnt4^{+/-}$ double heterozygous embryos were recovered in Mendelian ratios ($P = 0.97$; Fig. 4A).

Wild-type, $Sox7^{+/-}$, $Wnt4^{+/-}$, and $Sox7^{+/-}$;$Wnt4^{+/-}$ double heterozygous mice were not found in Mendelian ratios at weaning ($P = 0.0038$; Fig. 4B). Among the 107 progeny genotyped at weaning, 39.3% ($n = 42$) were wild-type, 23.4% ($n = 25$) were $Sox7^{+/-}$, 22.4% ($n = 24$) were $Wnt4^{+/-}$ and 15% ($n = 16$) were $Sox7^{+/-}$;$Wnt4^{+/-}$. This suggests that there is increased mortality among $Sox7^{+/-}$ and $Wnt4^{+/-}$ heterozygous mice and $Sox7^{+/-}$;$Wnt4^{+/-}$ double heterozygous mice between E15.5/E16.5 and weaning. The cause of this increased mortality is unclear. Although the number of double heterozygous mice recovered at weaning is lower than the number of heterozygotes recovered, this difference did not reach statistical significance ($P = 0.36$).

We then examined the hearts of E15.5 embryos with each of these genotypes. We found that 38% (3/8) of $Sox7^{+/-}$;$Wnt4^{+/-}$ embryos had VSDs. Two of the double heterozygous embryos had perimembranous VSDs (Fig. 4C), and one had a muscular VSD (Fig. 4D). No cardiac defects were identified in wild-type ($n = 8$), $Sox7^{+/-}$ ($n = 8$) or $Wnt4^{+/-}$ ($n = 8$) E15.5 embryo controls.

Sox7 and *Wnt4* interact genetically to reduce the mesenchymal cell density of the developing AV canal

To determine if the VSDs seen in $Sox7^{+/-}$;$Wnt4^{+/-}$ double heterozygous embryos at E15.5 were associated with hypocellularity of the AV endocardial cushions, as seen in $Sox7^{-/-}$ and

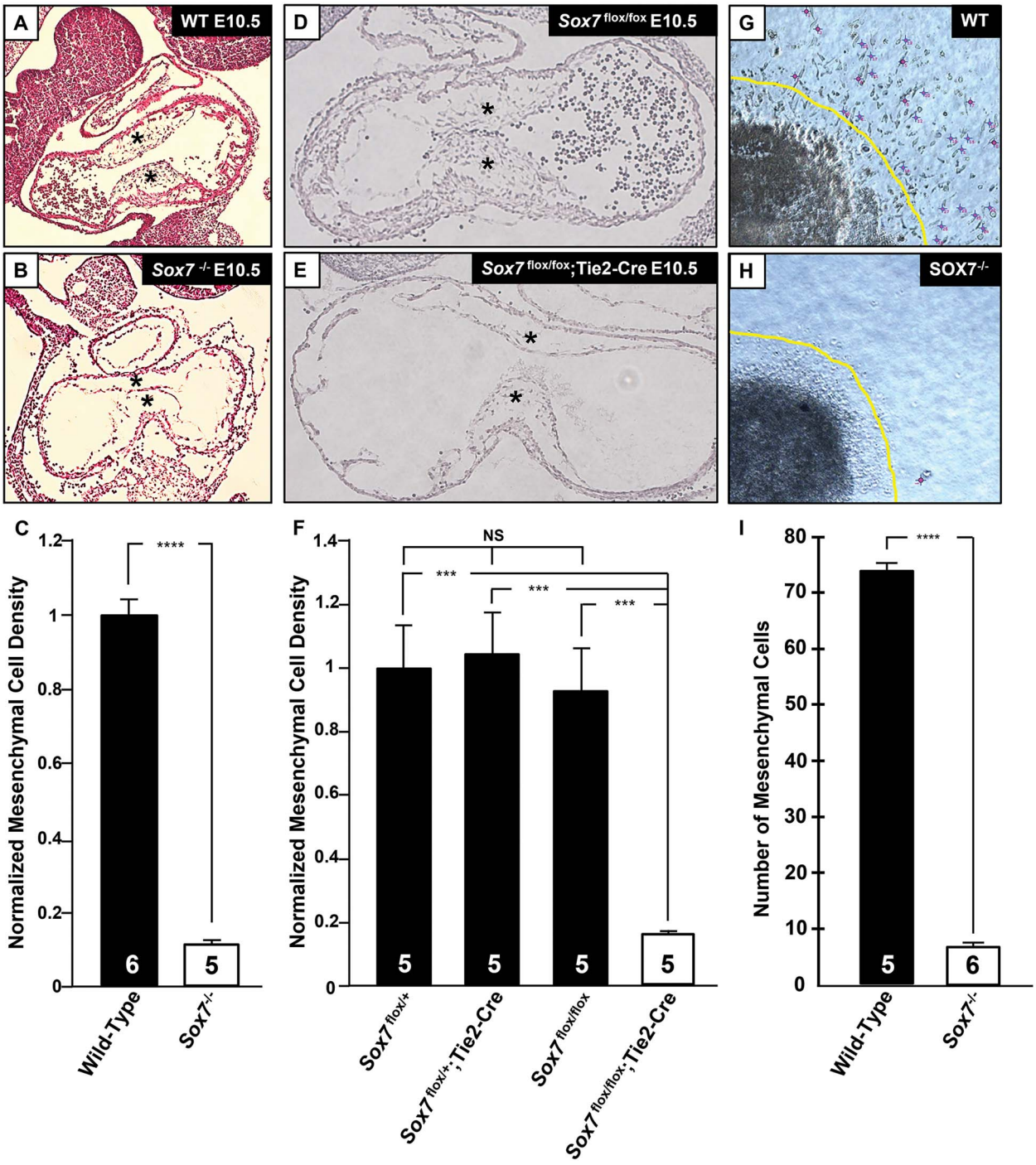

Figure 2. SOX7 deficiency leads to decreased mesenchymal cell density in the AV endocardial cushions because of decreased levels of EndMT. (**A**–**B**) At E10.5, the AV endocardial cushions of wild-type embryos are filled with mesenchymal cells (asterisks in A). In contrast, the AV endocardial cushions of $Sox7^{-/-}$ embryos harvested at E10.5 are hypocellular (asterisks in B). (**C**) E9.5/10.5 $Sox7^{-/-}$ embryos have significantly reduced mesenchymal cell density in their AV canals compared with wild-type embryos ($P \leq 0.0001$). (**D**–**E**) Hypocellular AV endocardial cushions (asterisks in E) were also seen in $Sox7^{flox/flox}$;Tie2-Cre embryos in which Sox7 was ablated specifically in the endocardium. (**F**) E10.5 $Sox7^{flox/flox}$;Tie2-Cre embryos had significantly reduced mesenchymal cell density in their AV canals compared with $Sox7^{flox/+}$, $Sox7^{flox/+}$;Tie2-Cre and $Sox7^{flox/flox}$ control embryos harvested at the same time point. (**G**–**I**) Collagen gel AV canal explants from E9.5 wild-type embryos generated a large number of migrating mesenchymal cells (marked by purple crosses). In contrast, collagen gel AV canal explants from $Sox7^{-/-}$ embryos generated a significantly reduced number of migrating mesenchymal cells ($P \leq 0.0001$). This suggests that SOX7 deficiency causes a severe defect in EndMT. Mesenchymal cell densities were calculated from 6–10 sagittal sections through the heart obtained from at least five embryos of each genotype which were then normalized on the basis of age-matched wild-type embryos. AV canal explant figures are representative images from explants obtained from five wild-type and six $Sox7^{-/-}$ embryos generated in crosses of $Sox7^{+/-}$ mice. Error bars represent the standard error of the mean. NS = not significant. $^{*}P \leq 0.05$, $^{**}P \leq 0.01$, $^{***}P \leq 0.001$, $^{****}P \leq 0.0001$.

$Sox7^{flox/flox}$;Tie2-Cre embryos, we compared the endocardial cushions of $Sox7^{+/-}$;$Wnt4^{+/-}$ embryos harvested at E10.5 with those of their wild-type, $Sox7^{+/-}$ and $Wnt4^{+/-}$ littermate controls. We found that the AV endocardial cushions of E10.5 $Sox7^{+/-}$;$Wnt4^{+/-}$ embryos had significantly reduced mesenchymal cell density compared with those of their control littermates (Fig. 4E). This

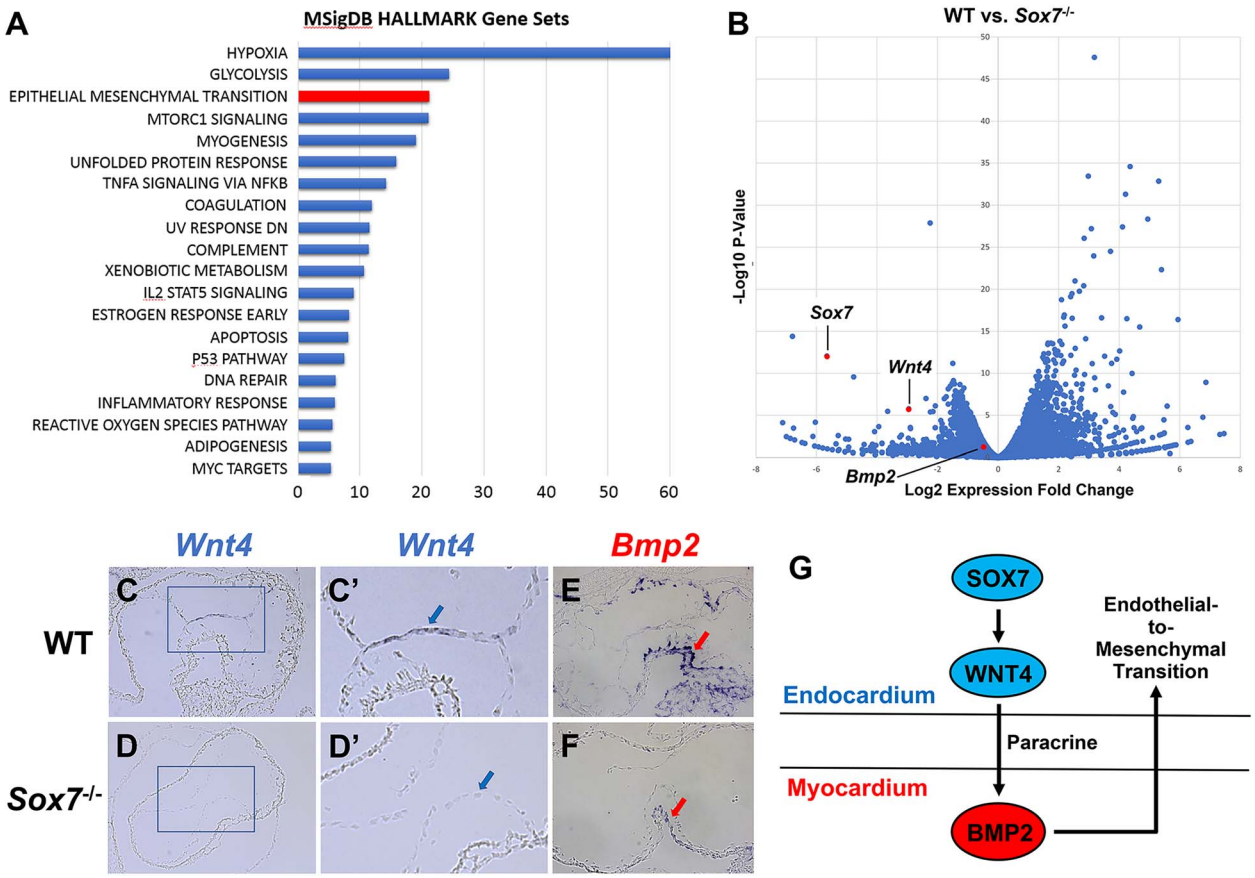

Figure 3. RNA-seq and RNA-ISH analyses of E9.5 wild-type and *Sox7*$^{-/-}$ heart tubes reveal perturbations in the expression of genes involved in epithelial-to-mesenchymal transition and a decrease in *Wnt4* and *Bmp2* transcripts. (**A**) MSigDB Hallmark gene set enrichments for 722 genes that were differentially expressed with *P*-value < 0.001 and absolute fold change > 2. (**B**) A volcano scatter plot representation of differentially expressed genes. We found significantly decreased levels of *Wnt4* expression in *Sox7*$^{-/-}$ heart tubes compared with those of wild-type embryos. The expression of *Bmp2*, WNT4's downstream target, was also diminished but not sufficiently to meet criteria for inclusion among the list of differentially expressed genes. (**C**–**C′**) RNA-ISH performed on sections obtained from E9.5 wild-type embryos demonstrates that *Wnt4* is expressed in the endocardium covering the AV endocardial cushions (blue arrow in magnified image C′). (**D**–**D′**) *Sox7*$^{-/-}$ embryos show reduced levels of *Wnt4* transcripts in the AV endocardium when compared with wild-type embryos (blue arrow in magnified image D′). (**E**–**F**) *Bmp2* transcripts are detected in the myocardium of the AV canal with reduced levels being seen in *Sox7*$^{-/-}$ embryos (red arrow in F) compared with wild-type controls (red arrow in E). (**G**) In our proposed model, SOX7 functions in the endocardium to positively regulate the expression of *Wnt4*. WNT4 acts as a paracrine factor to upregulate *Bmp2* expression in the myocardium (21). BMP2 then functions to induce EndMT in the AV canal (22). In *Sox7*$^{-/-}$ embryos, a defect in EndMT leads to the development of hypocellular AV endocardial cushions and ventricular septal defects. RNA-ISH figures are representative images from RNA-ISH studies performed on frozen sections obtained from four embryos of each genotype that were generated in crosses of *Sox7*$^{+/-}$ mice on a C57BL/6 background.

suggests that *Sox7* and *Wnt4* interact genetically to reduce the mesenchymal cell density of the endocardial cushions of the developing AV canal.

The mesenchymal cell density of the AV endocardial cushions of E10.5 *Wnt4*$^{+/-}$ embryos was also significantly reduced compared with those of wild-type and *Sox7*$^{+/-}$ embryos (Fig. 4E).

Discussion

CHD is present in over 1% of all newborns and is the leading cause of birth-defect-related deaths (23,24). Most CHD cases in the general population are thought to be caused by multiple genetic and environmental factors interacting in a multifactorial mode of inheritance (23). These types of interactions are difficult to study in the general population because of their complexity. One means of reducing this complexity is to study microdeletions in which the number of major CHD candidate genes is limited based on their location within a specific region.

8p23.1 microdeletion syndrome is associated with a high incidence of CHD with septal defects being particularly common (1). Although haploinsufficiency of *GATA4* is sufficient to cause CHD (6,7,25–27), clinical data suggest that haploinsufficiency of at least one additional gene in this region contributes to the development of CHD (1). Recently, Huang *et al*. described a four-generation family in which CHDs co-segregated with a c.310C>T, p.(Gln104*) [NM_031439.4] premature stop variant in *SOX7*. This report provided evidence that *SOX7* haploinsufficiency contributes to the development of CHD in individuals with 8p23.1 microdeletion syndrome and is sufficient to cause CHD in humans (8). Here, we used mouse models, collagen gel explant studies and RNA-seq transcriptome analysis to explore the morphogenetic and molecular mechanisms by which SOX7 deficiency causes septal defects in mice.

SOX7 deficiency in the endocardium leads to hypocellular AV cushions and VSDs through its effects on EndMT

The development of the AV cushions, which will ultimately give rise to the AV septum and its associated valves, requires multiple steps including cell commitment, deposition of the

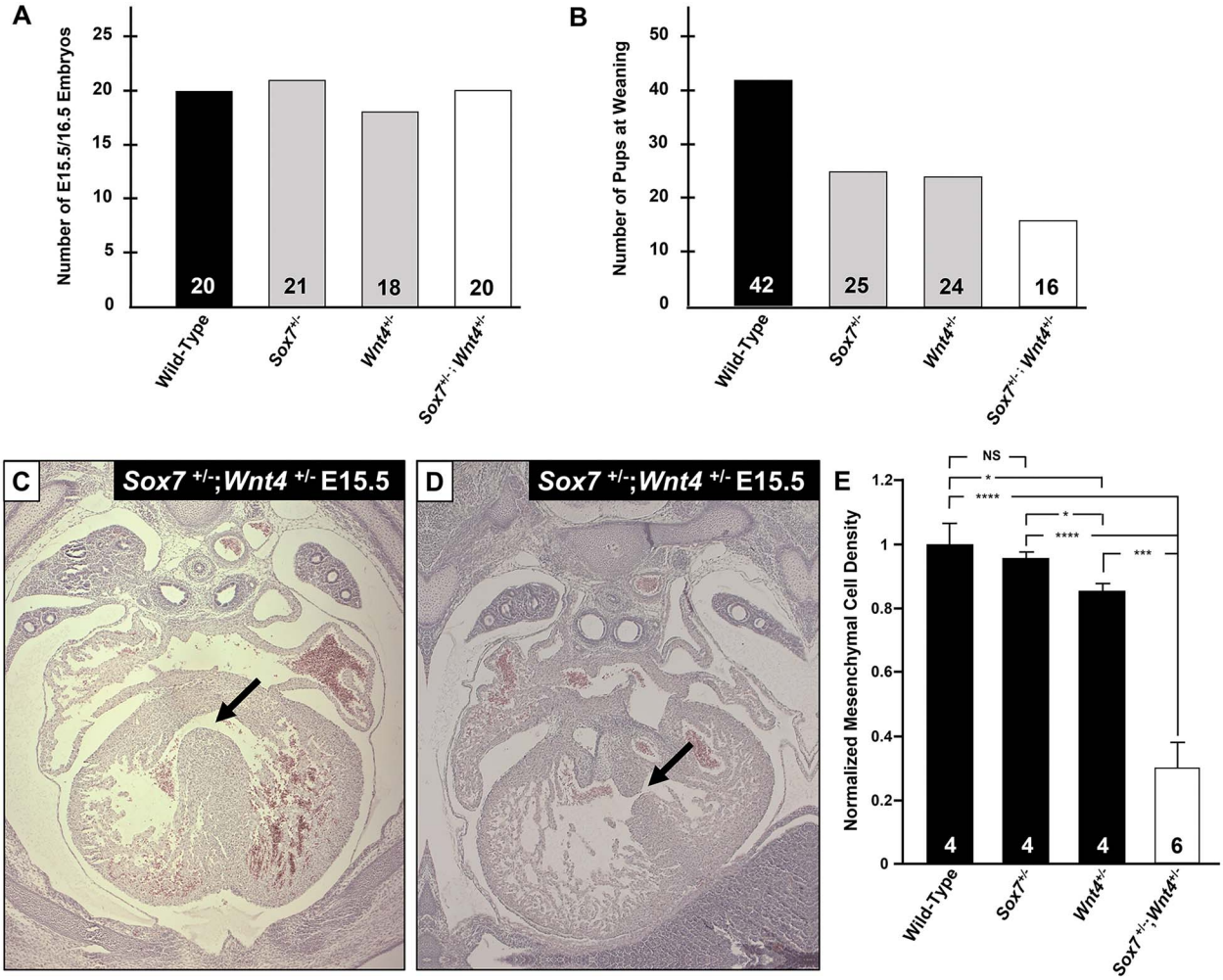

Figure 4. *Sox7* and *Wnt4* interact genetically in the formation of VSDs and hypocellular AV endocardial cushions. (**A**–**B**) Crosses between $Sox7^{+/-}$ and $Wnt4^{+/-}$ mice generated wild-type, $Sox7^{+/-}$, $Wnt4^{+/-}$ and $Sox7^{+/-}$;$Wnt4^{+/-}$ double heterozygous E15.5/E16.5 embryos in Mendelian ratios. In contrast, wild-type, $Sox7^{+/-}$, $Wnt4^{+/-}$, and $Sox7^{+/-}$;$Wnt4^{+/-}$ double heterozygous mice were not found in Mendelian ratios at weaning ($P = 0.0038$). Although the number of double heterozygous mice recovered at weaning is lower than the number of heterozygotes recovered, this difference was not statistically significant ($P = 0.36$). The cause of the increased mortality among $Sox7^{+/-}$ and $Wnt4^{+/-}$ heterozygous mice and $Sox7^{+/-}$;$Wnt4^{+/-}$ double heterozygous mice between E15.5/E16.5 and weaning is unclear. (**C**–**D**) 38% (3/8) $Sox7^{+/-}$;$Wnt4^{+/-}$ double heterozygous embryos develop perimembranous (black arrow in C) and muscular (black arrow in D) VSDs not seen in wild-type or $Sox7^{+/-}$ and $Wnt4^{+/-}$ heterozygous controls ($n = 8$ of each genotype). (**E**) The AV endocardial cushions of $Sox7^{+/-}$;$Wnt4^{+/-}$ embryos are hypocellular compared with those of wild-type, $Sox7^{+/-}$ and $Wnt4^{+/-}$ heterozygous controls. The mesenchymal cell density of the AV endocardial cushions of E10.5 $Wnt4^{+/-}$ embryos was also significantly reduced compared with those of wild-type and $Sox7^{+/-}$ embryos. Normalized mesenchymal cell densities were calculated on the basis of 10 sagittal sections through the heart obtained from at least four embryos of each genotype. Error bars represent the standard error of the mean. NS = not significant. $^{*}P \leq 0.05$, $^{***}P \leq 0.001$, $^{****}P \leq 0.0001$.

cardiac jelly, delamination of the endocardium, EndMT, and mesenchymal cell proliferation (28–32). We have shown that the AV cushions of $Sox7^{-/-}$ and $Sox7^{flox/flox}$;Tie2-Cre embryos at E10.5 have progressed successfully to the stage at which the endocardium separates from the underlying myocardium, and that the size of the AV endocardial cushions in these embryos is comparable to those of their wild-type littermates (Fig. 2A, B, D and E). However, these cushions are hypocellular (Fig. 2C and F), and $Sox7^{flox/-}$;Tie2-Cre and $Sox7^{flox/flox}$;Tie2-Cre embryos develop VSDs (Fig. 1), suggesting a defect in EndMT.

A severe defect in EndMT was confirmed in collagen explant studies in which there was a striking reduction in the number of migrating mesenchymal cells in $Sox7^{-/-}$ heart tube explants compared with explants from wild-type embryos (Fig. 2G–I). This leads us to conclude that the VSDs associated with SOX7 deficiency (Fig. 1) are due to an underlying defect in EndMT caused by loss of SOX7 function in endocardium.

SOX7 regulates EndMT through its effects on *Wnt4* transcription

Since SOX7 is an endocardially expressed DNA binding transcription factor (12,18,19), and its deficiency causes a severe defect in EndMT (Fig. 3), we hypothesized that it functions to regulate the transcription of genes that control EndMT. RNA-seq performed on wild-type and $Sox7^{-/-}$ E9.5 heart tubes (Fig. 3A and B) and RNA-ISH studies (Fig. 3C–F) revealed decreased expression of *Wnt4* in SOX7-deficient heart tubes. During the development of the AV endocardial cushions, WNT4 is expressed in the endocardium and acts as a paracrine factor to upregulate *Bmp2* expression in the adjacent myocardium (21). In turn, BMP2 functions to induce EndMT in the AV canal (22). Hence, our data are congruent with the model previously proposed by Hong *et al.* in which SOX7 modulates EndMT in the developing AV canal by modulating the expression of *Wnt4* and its downstream target gene, *Bmp2* (Fig. 3G) (13). This model is further supported by ChIP-qPCR and

luciferase assays performed by Hong *et al*. in which they demonstrate that SOX7 can bind to regions of the *Wnt4* promoter in both adult mouse hearts and in a mouse embryonic endocardial cells (MEECs) cell line and can activate the *Wnt4* promoter in MEECs (13).

Evidence that WNT4 and BMP2 play a role in ventricular septal development in humans

Systemic depletion of WNT4 expression in mice leads to perinatal death within 48 h associated with severe developmental anomalies of the kidneys, reproductive tract, and gonads (33–35). This is consistent with the phenotypes seen in individuals with Mullerian aplasia and hyperandrogenism [Mendelian inheritance in man (MIM)# 158330] who carry heterozygous missense variants in *WNT4* (36–38). We note that no cardiac phenotypes have been reported to date in WNT4-deficient mice, nor in individuals with Mullerian aplasia and hyperandrogenism.

Homozygous loss-of-function variants in *WNT4* have been reported in a single family to cause autosomal recessive 46,XX sex reversal with dysgenesis of kidney, adrenals and lungs (SERKAL) syndrome (MIM# 611812) whose features also include VSDs (39). We demonstrate that *Wnt4* haploinsufficiency causes decreased AV endocardial mesenchymal cell density (Fig. 4E), and that *Sox7* and *Wnt4* interact genetically in the development of hypocellular endocardial cushions (Fig. 4E) and perimembranous and muscular VSDs (Fig. 4C and D). This suggests that WNT4 deficiency plays an important role in mammalian cardiac development and provides supportive evidence that WNT4 deficiency can cause heart defects in the setting of SERKAL syndrome. Additional studies will be needed to confirm that loss of WNT4 function alone is sufficient to produce CHDs.

In contrast to WNT4, the role of BMP2 in mouse and human heart development has been clearly demonstrated. Studies performed in mice have shown that BMP2 is essential for EndMT in the AV canal and normal myocardial patterning (22). In humans, heterozygous pathogenic variants in *BMP2* cause short stature, facial dysmorphism and skeletal anomalies with or without cardiac anomalies 1 (SSFSC1) syndrome (MIM# 617877) (40). As expected from our studies, the cardiac defects seen in SSFSC1 syndrome include VSDs.

Taken together, our results provide additional evidence that SOX7, WNT4 and BMP2 function in the same signaling pathway during mammalian septal development, and that their deficiency can contribute to the development of VSDs in humans with 8p23.1 deletions, SERKAL syndrome, and SSFSC1 syndrome, respectively. Our results also suggest the possibility that combinations of deleterious *SOX7*, *WNT4* and *BMP2* alleles could contribute to the development of VSDs with an oligogenic or multifactorial mode of inheritance and underscore the importance of considering possible genetic interactions when reporting and interpreting genetic test results.

Materials and Methods

Mouse models

The generation of mice bearing *Sox7* conditional (flox) and null alleles were described previously (12). Briefly, the second exon of *Sox7*, which encodes half of SOX7's HMG-box DNA binding domain and the entire SOX7 activation domain, was flanked by loxP sites to generate the flox allele. In the presence of Cre, the second exon and the 3′ untranslated region are excised generating a null allele.

Mice bearing the *Wnt4* GCE knock-in/knock-out allele (*Wnt4*^{GCE}, Jackson Laboratory, strain #032489) have been previously described (41). This allele abolishes *Wnt4* gene function and expresses an EGFP and creERT2 (eGFPCreERT2) fusion protein from the *Wnt4* promoter/enhancer elements. In this manuscript, we refer to embryos and mice that are heterozygous for this allele as being *Wnt4*$^{+/-}$.

All mice in our study were maintained on a C57BL/6 background. All experiments using mouse models were conducted in accordance with the recommendations in the Guide for the Care and Use of Laboratory Animals of the National Institutes of Health. The associated protocols were approved by the Institutional Animal Care and Use Committee of Baylor College of Medicine (Animal Welfare Assurance #A3832-01).

Histology

For standard histology, embryos were fixed in buffered Formalde-Fresh Solution (Fisher) or 4% buffered paraformaldehyde (PFA). After fixation, the specimens were washed in phosphate-buffered saline (PBS), dehydrated in ethanol, embedded in paraffin and sectioned at 10 μm. Sections were then stained with hematoxylin and eosin.

Collagen gel explant assays

Collagen gel explant assays were performed as described by Xiong *et al*. (42). Briefly, collagen gels were prepared from a type I rat-tail collagen stock at ∼4 mg/ml (Corning). The solution was diluted with 1× PBS and buffered with 1 N NaOH. Collagen gels were soaked with culture medium containing OptiMEM-I (Gibco), 1% FBS (Thermo Fisher Scientific), 100 U/ml penicillin (Thermo Fisher Scientific) and 100 μg/ml streptomycin (Thermo Fisher Scientific) overnight at 37°C, and were allowed to solidify inside a 5% CO_2 incubator at 37°C. The culture medium was removed from the gels prior to the dissection of the AV canals.

E9.5 embryos with 20–25 pairs of somites were harvested in cold PBS. After removing the pericardial sac, AV canals were dissected and placed with the endocardium facing downwards on the surface of a collagen gel. Explants were incubated in 5% CO_2 at 37°C. Images were acquired at 48 h of culture using an Axiovert 40 CFL inverted microscope equipped with an AxioCam digital camera and imaging system (Carl Zeiss Microscopy).

Migratory mesenchymal cells (hypertrophied cells with elongated spindle-shaped morphology found growing out from the explant marginal area) were counted from explants obtained from wild-type and *Sox7*$^{-/-}$ embryos. An unpaired two-tailed Student's *t*-test was used to compare the numbers of migratory mesenchymal cells generated from explants of different genotypes.

E9.5 heart tube RNA isolation and RNA-seq analysis

Heart tubes were isolated from *Sox7*$^{-/-}$ embryos and their wild-type littermates at E9.5. Briefly, heart tubes were microdissected at the distal part of the outflow tract before it opens within the region of the aortic sac. Next, a lower slice was performed at the end of the common atrial chamber to obtain a heart segment including the endocardial cushions and the AV canal. Cephalic and tail poles were saved for genotyping. RNA was obtained from pools of ∼30–50 heart tubes of each genotype using an RNAeasy Plus Micro kit (QIAGEN) according to the manufacturer's instructions. RNA from two pooled *Sox7*$^{-/-}$ samples and one pooled wild-type sample were used for RNA-seq analyses.

Bulk RNA-Seq were performed at the Department of Molecular and Human Genetics Functional Genomics Core at Baylor College of Medicine. RNA-seq libraries ware made using a KAPA stranded mRNA-seq kit (KK8420). Briefly, poly-A RNA was purified from

total RNA using Oligo-dT beads, fragmented to a small size, after which the first-strand cDNA was synthesized. Second-strand cDNA was synthesized and marked with dUTP. The resultant cDNA was used for end repair, A-tailing, and adaptor ligation. Finally, libraries were amplified for sequencing using the Novaseq platform (Illumina). The strand marked with dUTP was not amplified, allowing strand-specific sequencing.

RNA-ISH

Embryos (E9.5) were collected, washed in cold PBS and fixed overnight in 4% PFA. After washing, the embryos were cryoprotected sequentially in PBS buffered 15% and 30% sucrose solutions, embedded in optimum cutting temperature compound (Tissue-Tek) and snap frozen. RNA-ISH was performed on serial 10 and 12 μm thick sections cut on a Leica CM3050 S cryostat. Sections were probed with digoxigenin-labeled sense and anti-sense mRNA probes. The *Wnt4* probe included an 800 bp sequence on the basis of NM_009523.2 flanked by forward 5′-CAGCATCTCCGAAGAGGAGAC-3′ and reverse 5′-CTTTAGATGTCTTGTTGCACG-3′ sequences. The *Bmp2* probe included a 259 bp region sequence on the basis of NM_007553.1 flanked by forward 5′-GATCTTCCGGGAACAGATACAG-3′ and reverse 5′-CACCTGGGTTCTCCTCTAAATG-3′ sequences as previously described in the Allen Brain Atlas (43). *In situ* hybridization was performed by the RNA *In Situ* Hybridization Core at Baylor College of Medicine using an automated robotic platform and a previously described protocol (44,45). Images were acquired using a Leica DM4000 microscope equipped with a Leica DMC 2900 camera (Leica Biosystems).

Statistics

Standard errors were calculated using the Standard Error Calculator from Good Calculators (https://goodcalculators.com/standard-error-calculator/). *P*-values were determined between categories using an unpaired *t*-test performed using the T-Test Calculator from GraphPad (https://www.graphpad.com/quickcalcs/ttest1.cfm). To determine if genotyping results were consistent with expected Mendelian ratios, we used a Chi-square test performed using the Chi-square test calculator from GraphPad (https://www.graphpad.com/quickcalcs/chisquared2/).

Supplementary Material

Supplementary Material is available at *HMG* online.

Acknowledgements

RNA-ISH was performed in the RNA *In Situ* Hybridization Core at Baylor College of Medicine. RNA-seq was performed in the Department of Molecular and Human Genetics Functional Genomics Core at Baylor College of Medicine.

Conflict of Interest statement. None.

Funding

National Institutes of Health [HD098458 to D.A.S. and a diversity supplement to A.M.B, OD016167 to M.C.L., OD023469 supported the Department of Molecular and Human Genetics Functional Genomics Core at Baylor College of Medicine, and the Eunice Kennedy Shriver National Institute of Child Health and Human Development/Intellectual and Developmental Disabilities Research Center, HD083092 supported the RNA *In Situ* Hybridization Core at Baylor College of Medicine]. A grant from The Cullen Foundation supported the work of K.E.P.

Data availability

The primary RNA-seq data associated with this manuscript has been submitted to the Gene Expression Omnibus (GEO) and can be accessed under the data accession ID GSE168543.

References

1. Wat, M.J., Shchelochkov, O.A., Holder, A.M., Breman, A.M., Dagli, A., Bacino, C., Scaglia, F., Zori, R.T., Cheung, S.W., Scott, D.A. and Kang, S.H.L. (2009) Chromosome 8p23.1 deletions as a cause of complex congenital heart defects and diaphragmatic hernia. *Am. J. Med. Genet. A*, **149A**, 1661–1677.
2. Devriendt, K., Matthijs, G., Van Dael, R., Gewillig, M., Eyskens, B., Hjalgrim, H., Dolmer, B., McGaughran, J., Brondum-Nielsen, K., Marynen, P. *et al.* (1999) Delineation of the critical deletion region for congenital heart defects, on chromosome 8p23.1. *Am. J. Hum. Genet.*, **64**, 1119–1126.
3. Shimokawa, O., Miyake, N., Yoshimura, T., Sosonkina, N., Harada, N., Mizuguchi, T., Kondoh, S., Kishino, T., Ohta, T., Remco, V. *et al.* (2005) Molecular characterization of del(8)(p23.1p23.1) in a case of congenital diaphragmatic hernia. *Am. J. Med. Genet. A*, **136**, 49–51.
4. Lopez, I., Bafalliu, J.A., Bernabe, M.C., Garcia, F., Costa, M. and Guillen-Navarro, E. (2006) Prenatal diagnosis of de novo deletions of 8p23.1 or 15q26.1 in two fetuses with diaphragmatic hernia and congenital heart defects. *Prenat. Diagn.*, **26**, 577–580.
5. Slavotinek, A., Lee, S.S., Davis, R., Shrit, A., Leppig, K.A., Rhim, J., Jasnosz, K., Albertson, D. and Pinkel, D. (2005) Fryns syndrome phenotype caused by chromosome microdeletions at 15q26.2 and 8p23.1. *J. Med. Genet.*, **42**, 730–736.
6. Garg, V., Kathiriya, I.S., Barnes, R., Schluterman, M.K., King, I.N., Butler, C.A., Rothrock, C.R., Eapen, R.S., Hirayama-Yamada, K., Joo, K. *et al.* (2003) GATA4 mutations cause human congenital heart defects and reveal an interaction with TBX5. *Nature*, **424**, 443–447.
7. Okubo, A., Miyoshi, O., Baba, K., Takagi, M., Tsukamoto, K., Kinoshita, A., Yoshiura, K., Kishino, T., Ohta, T., Niikawa, N. and Matsumoto, N. (2004) A novel GATA4 mutation completely segregated with atrial septal defect in a large Japanese family. *J. Med. Genet.*, **41**, e97.
8. Huang, R.T., Guo, Y.H., Yang, C.X., Gu, J.N., Qiu, X.B., Shi, H.Y., Xu, Y.J., Xue, S. and Yang, Y.Q. (2022) SOX7 loss-of-function variation as a cause of familial congenital heart disease. *Am. J. Transl. Res.*, **14**, 1672–1684.
9. Zhang, C., Basta, T. and Klymkowsky, M.W. (2005) SOX7 and SOX18 are essential for cardiogenesis in Xenopus. *Dev. Dyn.*, **234**, 878–891.
10. Pendeville, H., Winandy, M., Manfroid, I., Nivelles, O., Motte, P., Pasque, V., Peers, B., Struman, I., Martial, J.A. and Voz, M.L. (2008) Zebrafish Sox7 and Sox18 function together to control arterial-venous identity. *Dev. Biol.*, **317**, 405–416.
11. Herpers, R., van de Kamp, E., Duckers, H.J. and Schulte-Merker, S. (2008) Redundant roles for sox7 and sox18 in arteriovenous specification in zebrafish. *Circ. Res.*, **102**, 12–15.
12. Wat, M.J., Beck, T.F., Hernandez-Garcia, A., Yu, Z., Veenma, D., Garcia, M., Holder, A.M., Wat, J.J., Chen, Y., Mohila, C.A. *et al.* (2012) Mouse model reveals the role of SOX7 in the development

of congenital diaphragmatic hernia associated with recurrent deletions of 8p23.1. *Hum. Mol. Genet.*, **21**, 4115–4125.
13. Hong, N., Zhang, E., Xie, H., Jin, L., Zhang, Q., Lu, Y., Chen, A.F., Yu, Y., Zhou, B., Chen, S., Yu, Y. and Sun, K. (2021) The transcription factor Sox7 modulates endocardiac cushion formation contributed to atrioventricular septal defect through Wnt4/Bmp2 signaling. *Cell Death Dis.*, **12**, 393.
14. Kisanuki, Y.Y., Hammer, R.E., Miyazaki, J., Williams, S.C., Richardson, J.A. and Yanagisawa, M. (2001) Tie2-Cre transgenic mice: a new model for endothelial cell-lineage analysis in vivo. *Dev. Biol.*, **230**, 230–242.
15. Anderson, R.H., Webb, S., Brown, N.A., Lamers, W. and Moorman, A. (2003) Development of the heart: (2) septation of the atriums and ventricles. *Heart*, **89**, 949–958.
16. Markwald, R.R., Krook, J.M., Kitten, G.T. and Runyan, R.B. (1981) Endocardial cushion tissue development: structural analyses on the attachment of extracellular matrix to migrating mesenchymal cell surfaces. *Scan. Electron Microsc.*, **2**, 261–274.
17. Armstrong, E.J. and Bischoff, J. (2004) Heart valve development: endothelial cell signaling and differentiation. *Circ. Res.*, **95**, 459–470.
18. Taniguchi, K., Hiraoka, Y., Ogawa, M., Sakai, Y., Kido, S. and Aiso, S. (1999) Isolation and characterization of a mouse SRY-related cDNA, mSox7. *Biochim. Biophys. Acta*, **1445**, 225–231.
19. Takash, W., Canizares, J., Bonneaud, N., Poulat, F., Mattei, M.G., Jay, P. and Berta, P. (2001) SOX7 transcription factor: sequence, chromosomal localisation, expression, transactivation and interference with Wnt signalling. *Nucleic Acids Res.*, **29**, 4274–4283.
20. Subramanian, A., Tamayo, P., Mootha, V.K., Mukherjee, S., Ebert, B.L., Gillette, M.A., Paulovich, A., Pomeroy, S.L., Golub, T.R., Lander, E.S. and Mesirov, J.P. (2005) Gene set enrichment analysis: a knowledge-based approach for interpreting genome-wide expression profiles. *Proc. Natl. Acad. Scie.U.S.A.*, **102**, 15545–15550.
21. Wang, Y., Wu, B., Chamberlain, A.A., Lui, W., Koirala, P., Susztak, K., Klein, D., Taylor, V. and Zhou, B. (2013) Endocardial to myocardial notch-wnt-bmp axis regulates early heart valve development. *PLoS One*, **8**, e60244.
22. Ma, L., Lu, M.F., Schwartz, R.J. and Martin, J.F. (2005) Bmp2 is essential for cardiac cushion epithelial-mesenchymal transition and myocardial patterning. *Development*, **132**, 5601–5611.
23. Pierpont, M.E., Basson, C.T., Benson, D.W., Jr., Gelb, B.D., Giglia, T.M., Goldmuntz, E., McGee, G., Sable, C.A., Srivastava, D. and Webb, C.L. (2007) Genetic basis for congenital heart defects: current knowledge: a scientific statement from the American Heart Association Congenital Cardiac Defects Committee, Council on Cardiovascular Disease in the Young: endorsed by the American Academy of Pediatrics. *Circulation*, **115**, 3015–3038.
24. Gilboa, S.M., Salemi, J.L., Nembhard, W.N., Fixler, D.E. and Correa, A. (2010) Mortality resulting from congenital heart disease among children and adults in the United States, 1999 to 2006. *Circulation*, **122**, 2254–2263.
25. Pehlivan, T., Pober, B.R., Brueckner, M., Garrett, S., Slaugh, R., Van Rheeden, R., Wilson, D.B., Watson, M.S. and Hing, A.V. (1999) GATA4 haploinsufficiency in patients with interstitial deletion of chromosome region 8p23.1 and congenital heart disease. *Am. J. Med. Genet.*, **83**, 201–206.
26. Reamon-Buettner, S.M. and Borlak, J. (2005) GATA4 zinc finger mutations as a molecular rationale for septation defects of the human heart. *J. Med. Genet.*, **42**, e32.
27. Sarkozy, A., Conti, E., Neri, C., D'Agostino, R., Digilio, M.C., Esposito, G., Toscano, A., Marino, B., Pizzuti, A. and Dallapiccola, B. (2005) Spectrum of atrial septal defects associated with mutations of NKX2.5 and GATA4 transcription factors. *J. Med. Genet.*, **42**, e16.
28. Kaneko, K., Li, X., Zhang, X., Lamberti, J.J., Jamieson, S.W. and Thistlethwaite, P.A. (2008) Endothelial expression of bone morphogenetic protein receptor type 1a is required for atrioventricular valve formation. *Ann. Thorac. Surg.*, **85**, 2090–2098.
29. Rivera-Feliciano, J. and Tabin, C.J. (2006) Bmp2 instructs cardiac progenitors to form the heart-valve-inducing field. *Dev. Biol.*, **295**, 580–588.
30. Combs, M.D. and Yutzey, K.E. (2009) Heart valve development: regulatory networks in development and disease. *Circ. Res.*, **105**, 408–421.
31. Eisenberg, L.M. and Markwald, R.R. (1995) Molecular regulation of atrioventricular valvuloseptal morphogenesis. *Circ. Res.*, **77**, 1–6.
32. Lin, C.J., Lin, C.Y., Chen, C.H., Zhou, B. and Chang, C.P. (2012) Partitioning the heart: mechanisms of cardiac septation and valve development. *Development*, **139**, 3277–3299.
33. Boyer, A., Lapointe, E., Zheng, X., Cowan, R.G., Li, H., Quirk, S.M., DeMayo, F.J., Richards, J.S. and Boerboom, D. (2010) WNT4 is required for normal ovarian follicle development and female fertility. *FASEB J.*, **24**, 3010–3025.
34. Stark, K., Vainio, S., Vassileva, G. and McMahon, A.P. (1994) Epithelial transformation of metanephric mesenchyme in the developing kidney regulated by Wnt-4. *Nature*, **372**, 679–683.
35. Vainio, S., Heikkila, M., Kispert, A., Chin, N. and McMahon, A.P. (1999) Female development in mammals is regulated by Wnt-4 signalling. *Nature*, **397**, 405–409.
36. Biason-Lauber, A., De Filippo, G., Konrad, D., Scarano, G., Nazzaro, A. and Schoenle, E.J. (2007) WNT4 deficiency—a clinical phenotype distinct from the classic Mayer–Rokitansky–Kuster–Hauser syndrome: a case report. *Hum. Reprod.*, **22**, 224–229.
37. Biason-Lauber, A., Konrad, D., Navratil, F. and Schoenle, E.J. (2004) AWNT4Mutation associated with Müllerian-duct regression and virilization in a 46,XX woman. *N. Engl. J. Med.*, **351**, 792–798.
38. Philibert, P., Biason-Lauber, A., Rouzier, R., Pienkowski, C., Paris, F., Konrad, D., Schoenle, E. and Sultan, C. (2008) Identification and functional analysis of a new WNT4 gene mutation among 28 adolescent girls with primary amenorrhea and mullerian duct abnormalities: a French collaborative study. *J. Clin. Endocrinol. Metab.*, **93**, 895–900.
39. Mandel, H., Shemer, R., Borochowitz, Z.U., Okopnik, M., Knopf, C., Indelman, M., Drugan, A., Tiosano, D., Gershoni-Baruch, R., Choder, M. and Sprecher, E. (2008) SERKAL syndrome: an autosomal-recessive disorder caused by a loss-of-function mutation in WNT4. *Am. J. Hum. Genet.*, **82**, 39–47.
40. Tan, T.Y., Gonzaga-Jauregui, C., Bhoj, E.J., Strauss, K.A., Brigatti, K., Puffenberger, E., Li, D., Xie, L., Das, N., Skubas, I. *et al.* (2017) Monoallelic BMP2 variants predicted to result in haploinsufficiency cause craniofacial, skeletal, and cardiac features overlapping those of 20p12 deletions. *Am. J. Hum. Genet.*, **101**, 985–994.
41. Kobayashi, A., Valerius, M.T., Mugford, J.W., Carroll, T.J., Self, M., Oliver, G. and McMahon, A.P. (2008) Six2 defines and regulates a multipotent self-renewing nephron progenitor population throughout mammalian kidney development. *Cell Stem Cell*, **3**, 169–181.

42. Xiong, Y., Zhou, B. and Chang, C.-P. (2012) Analysis of the endocardial-to-mesenchymal transformation of heart valve development by collagen gel culture assay. In Peng, X. and Antonyak, M. (eds), *Cardiovascular Development: Methods and Protocols*. Humana Press, Totowa, NJ, pp. 101–109.
43. Lein, E.S., Hawrylycz, M.J., Ao, N., Ayres, M., Bensinger, A., Bernard, A., Boe, A.F., Boguski, M.S., Brockway, K.S., Byrnes, E.J. *et al.* (2007) Genome-wide atlas of gene expression in the adult mouse brain. *Nature*, **445**, 168–176.
44. Yaylaoglu, M.B., Titmus, A., Visel, A., Alvarez-Bolado, G., Thaller, C. and Eichele, G. (2005) Comprehensive expression atlas of fibroblast growth factors and their receptors generated by a novel robotic in situ hybridization platform. *Dev. Dyn.*, **234**, 371–386.
45. White, J.J., Arancillo, M., Stay, T.L., George-Jones, N.A., Levy, S.L., Heck, D.H. and Sillitoe, R.V. (2014) Cerebellar zonal patterning relies on Purkinje cell neurotransmission. *J. Neurosci.*, **34**, 8231–8245.